Coverage Enhancement in Disaster Communication Networks via Active RIS-Assisted UAV Deployment

Yong-Jin Song*, Juyeong Baek*, Hyungsub Kim†, Jeehyeon Na†,
Jung-Mo Moon†, Minsoo Jeong†, Howon Lee‡, and Bang Chul Jung‡
Department of Artificial Intelligence Convergence Network, Ajou University, Suwon, 16499, South Korea
†Electronics and Telecommunication Research Institute, ETRI, Daejeon, South Korea
‡Department of Electrical and Computer Engineering, Ajou University, Suwon, 16499, South Korea
Email: *{wiclyjsong, jybaek}@ajou.ac.kr, †{mobman, jhna, jmmoon, qwjms}@etri.re.kr, ‡{howon, bcjung}@ajou.ac.kr

***Abstract*—In this paper, we investigate an active Reconfigurable Intelligent Surface (RIS)-assisted unmanned aerial vehicle base station (UAV-BS) system for disaster communication networks. To mitigate the cascaded path loss in the UAV–RIS–user equipment (UE) link, an active RIS capable of amplifying reflected signals is employed. The coverage performance is evaluated and compared with three benchmark architectures: UAV-BS-only, passive RIS-assisted, and amplify-and-forward (AF) relay-assisted systems. Simulation results demonstrate that the active RIS significantly improves the coverage probability and effectively restores the coverage of the failed base station in disaster environments.**

***Index Terms*—Reconfigurable intelligent surface (RIS), unmanned aerial vehicle (UAV), disaster communication networks, coverage probability.**

I. Introduction

Natural disasters can severely damage terrestrial communication networks, causing widespread service outages and loss of connectivity. In such situations, rapidly restoring communication services is critical for rescue operations, situational awareness, and emergency response [1]. Recently, unmanned aerial vehicles (UAVs) have attracted significant attention as an effective solution for providing temporary communication services in disaster environments due to their high mobility, flexible deployment capability, and high probability of establishing line-of-sight (LoS) links with ground user equipments (UEs) [2]. In particular, UAV-mounted aerial base stations (UAV-BSs) have been widely investigated as a promising technology for quickly restoring communication coverage by replacing damaged terrestrial base stations [3]. However, relying solely on UAV-based aerial base stations may not guarantee reliable communication in disaster environments. Propagation loss and blockage can significantly degrade UAV-to-UE links, leaving some UEs with weak received signals and limiting the overall coverage performance.

To mitigate these issues, Reconfigurable Intelligent Surface (RIS) technology has recently emerged as a promising approach [4]. RIS can create an additional reflected path between the transmitter and the receiver, thereby enhancing the received signal power. However, passive RIS architectures only adjust the phase of the incident signal without amplification, which leads to severe cascaded path loss and may significantly limit the achievable performance, particularly under weak incident signal conditions.

To address this limitation, active RIS has recently been proposed as a promising alternative. Unlike passive RIS, active RIS incorporates amplification circuits within its reflecting elements, enabling the reflected signal to be amplified before being retransmitted [5]. This capability allows active RIS to generate stronger reflected signals even under weak incident signal conditions, thereby mitigating the severe cascaded path loss in UAV-assisted links. Moreover, signal amplification makes active RIS less sensitive to placement conditions than passive RIS, enabling more stable transmission performance [6]. [7] compared the performance of passive RIS and active RIS in a post-disaster communication scenario within a High-Altitude Platform Station (HAPS)-RIS-assisted Internet of Things (IoT) network. However, studies on the use of active RIS in disaster communication networks remain limited.

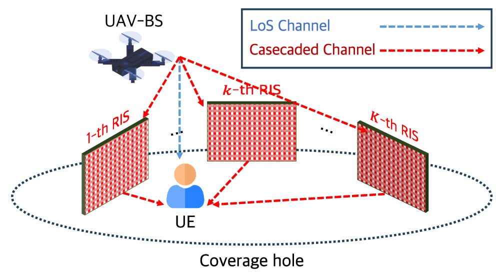

Fig. 1. System model of the proposed disaster-recovery network with a single UAV-BS, K active RIS panels, and a single UE.

In this paper, we investigate an active RIS-assisted UAV-BS communication architecture for post-disaster environments. The proposed architecture aims to enhance coverage performance by mitigating the severe cascaded path loss in UAV-assisted links. To evaluate the effectiveness of the proposed active RIS architecture, it is compared with three benchmark architectures: UAV-BS-only, passive RIS-assisted, and amplify-and-forward (AF) relay-assisted. The simulation results show that the proposed active RIS architecture significantly improves coverage performance compared with the benchmark architectures in disaster environments.

II. System Model

In this paper, we consider a downlink disaster-recovery communication system where the terrestrial BS is assumed to be non-operational due to a disaster. To restore the failed coverage, a single UAV-BS is deployed to serve a ground UE. To further enhance the communication reliability and coverage, K active RIS panels are additionally deployed to assist the UAV-BS–UE transmission. For simplicity, the UAV-BS and the UE are assumed to be equipped with a single isotropic antennas, and each RIS element is assumed to exhibit an isotropic reflection pattern, such that antenna gain and radiation pattern effects are omitted.

We consider a three-dimensional Cartesian coordinate system. The UAV-BS and the UE are located at $\mathbf{q}_{\mathrm{B}} = [x_{\mathrm{B}}, y_{\mathrm{B}}, h_{\mathrm{UAV}}]^{\mathrm{T}}$, $\mathbf{q}_{\mathrm{U}} = [x_{\mathrm{U}}, y_{\mathrm{U}}, 1.5]^{\mathrm{T}}$. $(\cdot)^{\mathrm{T}}$ denotes the transpose operator. The center position of the k-th active RIS panel is denoted as $\mathbf{q}_{\mathrm{R},k} = [x_{\mathrm{R},k}, y_{\mathrm{R},k}, h_{\mathrm{R},k}]^{\mathrm{T}}$, $k \in \mathcal{K} \triangleq \{1, \ldots, K\}$, where $\mathbf{q}_{\mathrm{R},k}$ represents the geometric center of the k-th RIS panel. Each RIS panel consists of $M \times N$ reflecting elements with element size $d_x \times d_y$, $d_x = d_y = \lambda/2$. λ is the wavelength. Let $\mathbf{e}_{k,1}$ and $\mathbf{e}_{k,2}$ denote two orthogonal basis vectors spanning the surface of the k-th RIS panel. Then, the unit normal vector of the panel is given by $\mathbf{n}_k = \mathbf{e}_{k,1} \times \mathbf{e}_{k,2}$, with $\mathbf{e}_{k,1}^{\mathrm{T}} \mathbf{e}_{k,2} = 0$, $\|\mathbf{e}_{k,1}\| = \|\mathbf{e}_{k,2}\| = \|\mathbf{n}_k\| = 1$. $\mathbf{e}_1 = \frac{\mathbf{z} \times \mathbf{n}}{\|\mathbf{z} \times \mathbf{n}\|}$, where $\mathbf{z} = [0, 0, 1]^{\mathrm{T}}$. For the (m, n)-th element of the k-th RIS panel, its local two-dimensional position vector with respect to the panel center is defined as

$$\mathbf{u}_{k,m,n} = \left(m - \frac{M+1}{2} \right) d_x \mathbf{e}_{k,1} + \left(n - \frac{N+1}{2} \right) d_y \mathbf{e}_{k,2}, \quad (1)$$

where $m \in \{1, \ldots, M\}$ and $n \in \{1, \ldots, N\}$. Accordingly, the three-dimensional position vector of the (m, n)-th element is given by $\mathbf{q}_{\mathrm{R},k,m,n} = \mathbf{q}_{\mathrm{R},k} + \mathbf{u}_{k,m,n}$. The UAV-BS–UE distance is $d_{\mathrm{BU}} = \|\mathbf{q}_{\mathrm{B}} - \mathbf{q}_{\mathrm{U}}\|$. The distances from the UAV-BS to the center of the k-th RIS panel and from the center of the k-th RIS panel to the UE are $d_{\mathrm{BR},k} = \|\mathbf{q}_{\mathrm{B}} - \mathbf{q}_{\mathrm{R},k}\|$, $d_{\mathrm{RU},k} = \|\mathbf{q}_{\mathrm{U}} - \mathbf{q}_{\mathrm{R},k}\|$, respectively.

The direct link between the UAV-BS and the UE is assumed to be dominated by a LoS component and is modeled as

$$h_{\mathrm{D}} = \frac{\lambda}{4\pi \sqrt{d_{\mathrm{BU}}^{\alpha_{\mathrm{D}}}}} e^{-j \frac{2\pi}{\lambda} d_{\mathrm{BU}}}, \quad (2)$$

where α_{D} is the path-loss exponent of the direct link. For the (m, n)-th element of the k-th RIS panel, let $D_{k,m,n} = \|\mathbf{q}_{\mathrm{B}} - \mathbf{q}_{\mathrm{R},k,m,n}\|$ and $d_{k,m,n} = \|\mathbf{q}_{\mathrm{U}} - \mathbf{q}_{\mathrm{R},k,m,n}\|$ be the UAV-BS–to–RIS and RIS–to–UE distances, respectively. Then, the cascaded channel through the (m, n)-th element is expressed as

$$h_{k,m,n} = \frac{\lambda \sqrt{d_x d_y}}{(4\pi)^{3/2} \sqrt{D_{k,m,n}^{\alpha_1} d_{k,m,n}^{\alpha_2}}} \times \eta_{k,m,n} e^{-j \frac{2\pi}{\lambda} (D_{k,m,n} + d_{k,m,n}) + \phi_{k,m,n}}, \quad (3)$$

where $\eta_{k,m,n} \geq 1$ denotes the amplitude gain of the (m, n)-th active RIS element, $\phi_{k,m,n}$ denotes the applied phase shift, and α_1 and α_2 represent the path-loss exponents of the UAV-BS–RIS and RIS–UE links, respectively. To coherently combine the reflected signal with the direct LoS component, the RIS phase shift is designed to compensate for the phase difference between the direct path and the cascaded path. Therefore, the phase shift of the (m, n)-th element in the k-th RIS panel is set as $\phi_{k,m,n}^{\star} = \mathrm{mod}\big(\frac{2\pi}{\lambda}\big(D_{k,m,n} + d_{k,m,n} - d_{\mathrm{BU}}\big), 2\pi\big)$, where $\mathrm{mod}(a, b)$ maps a to the interval $[0, b)$. With this phase design, the reflected signal from each RIS element is aligned with the phase of the direct UAV-BS–UE link.

The total available power budget is shared by the UAV-BS and all active RIS panels as

$$P_{\mathrm{total}} = P_{\mathrm{UAV}} + \sum_{k=1}^{K} P_{\mathrm{RIS},k}, \quad (4)$$

TABLE I: Simulation Parameters

Parameter	Value
Carrier frequency	2.1 GHz
System bandwidth	20 MHz
Cell radius	1 km
UAV-BS position $\mathbf{q}_{\mathrm{B}}$	$[0, 0, 35]^{\mathrm{T}}$ m
Auxiliary node height h_{aux}	20 m
Horizontal distance d_{aux}	30 m
No. of auxiliary nodes K	4
UAV transmit power P_{UAV}	5 W
Noise spectral density N_0	-174 dBm/Hz
Target SNR threshold γ_{th}	7 dB
Path-loss exponent $(\alpha_{\mathrm{D}}, \alpha_1, \alpha_2)$	$(2.2, 2.2, 3)$

where P_{UAV} and $P_{\mathrm{RIS},k}$ represent the UAV-BS transmit power and the power consumed by the k-th active RIS panel, respectively. Since each panel contains MN active elements and each element consumes amplification power P_{amp}, we have $P_{\mathrm{RIS},k} = MN\, P_{\mathrm{amp}}$, and thus $P_{\mathrm{aux}} = \sum_{k=1}^{K} P_{\mathrm{RIS},k} = KMN\, P_{\mathrm{amp}}$. Therefore, the received signal at the UE is expressed as

$$y = \left(h_{\mathrm{D}} + \sum_{k=1}^{K} h_{\mathrm{RIS},k} \right) \sqrt{P_{\mathrm{UAV}}}\, x + \sum_{k=1}^{K} \sum_{m=1}^{M} \sum_{n=1}^{N} \tilde{h}_{k,m,n}\, z_{k,m,n} + n_{\mathrm{U}}, \quad (5)$$

where $z_{k,m,n} \sim \mathcal{CN}(0, \sigma_{z,k,m,n}^2)$ denotes the amplification noise introduced by the (m, n)-th element of the k-th active RIS panel, and $n_{\mathrm{U}} \sim \mathcal{CN}(0, \sigma_{\mathrm{U}}^2)$ is the additive white Gaussian noise at the UE. The effective reflected channel of the k-th RIS panel is then written as $h_{\mathrm{RIS},k} = \sum_{m=1}^{M} \sum_{n=1}^{N} h_{k,m,n}$. The equivalent channel from the (m, n)-th element of the k-th active RIS panel to the UE for the amplification noise is defined as

$$\tilde{h}_{k,m,n} = \frac{\lambda \sqrt{d_x d_y}}{(4\pi)^{3/2} \sqrt{d_{k,m,n}^{\alpha_2}}} \eta_{k,m,n} e^{-j \frac{2\pi}{\lambda} d_{k,m,n} + \phi_{k,m,n}}. \quad (6)$$

Moreover, x is the normalized information symbol satisfying $\mathbb{E}[|x|^2] = 1$. Accordingly, the received signal-to-interference-plus-noise ratio (SINR) is given by

$$\gamma = \frac{P_{\mathrm{UAV}} \left| h_{\mathrm{D}} + \sum_{k=1}^{K} h_{\mathrm{RIS},k} \right|^2}{\sum_{k=1}^{K} \sum_{m=1}^{M} \sum_{n=1}^{N} |\tilde{h}_{k,m,n}|^2 \sigma_{z,k,m,n}^2 + \sigma_{\mathrm{U}}^2}. \quad (7)$$

The coverage probability is defined as the probability that the received SINR exceeds the target threshold γ_{th}, i.e.,

$$P_{\mathrm{cov}} = \Pr(\gamma \geq \gamma_{\mathrm{th}}), \quad (8)$$

where $\Pr(\cdot)$ denotes the probability operator.

III. Simulation Results

In this section, we evaluate the coverage performance of the considered UAV-BS-assisted disaster recovery architecture with active RIS support. In this paper, we consider a hexagonal cellular layout. To assist the UAV-BS transmission, four auxiliary nodes are deployed symmetrically around the origin along the x- and y-axes. Depending on the architecture considered, these auxiliary nodes correspond to AF relays, passive RIS panels, or active RIS panels. Their locations

TABLE II: Simulation Scenarios

Case	Architecture	P_{aux} (mW)	$M \times N$
1	UAV-BS only	0	–
2	AF relay	12.5	–
3	AF relay	320	–
4	Passive RIS	–	8×8
5	Passive RIS	–	8×16
6	Passive RIS	–	16×16
7	Active RIS	0.047	8×8
8	Active RIS	0.093	8×8
9	Active RIS	0.233	8×8
10	Active RIS	2.325	8×8

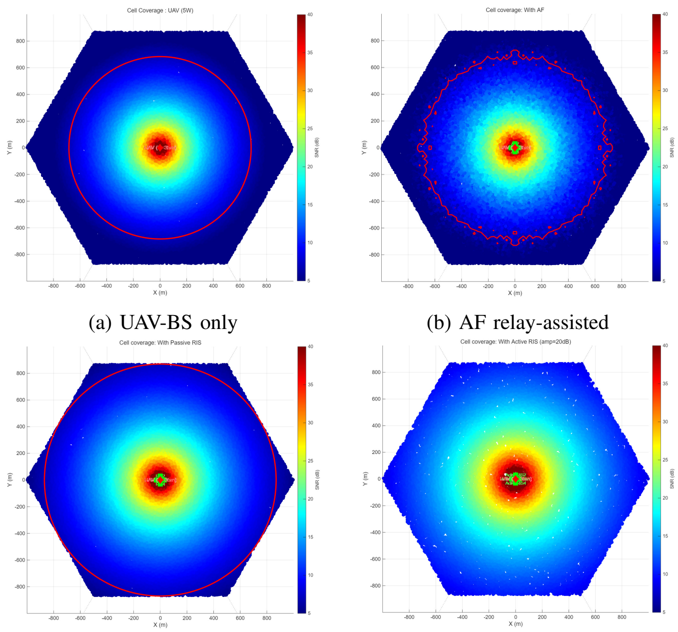

(a) UAV-BS only (b) AF relay-assisted

(c) Passive RIS-assisted (d) Active RIS-assisted

Fig. 2. Coverage probability comparison for different transmission architectures.

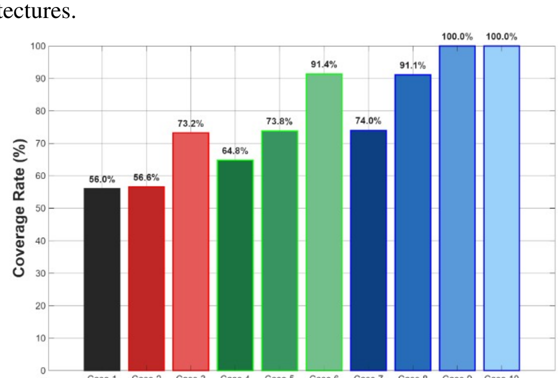

Fig. 3. Coverage rate comparison for different transmission architectures.

are given by $(d_{\text{aux}}, 0, h_{\text{aux}})$, $(-d_{\text{aux}}, 0, h_{\text{aux}})$, $(0, d_{\text{aux}}, h_{\text{aux}})$, and $(0, -d_{\text{aux}}, h_{\text{aux}})$. For RIS-assisted architectures, each RIS panel is assumed to face the UAV-BS. We set the normal vector of the k-th RIS as $\mathbf{n}_k = \frac{\mathbf{q}_{\text{U}} - \mathbf{q}_{\text{R},k}}{\|\mathbf{q}_{\text{U}} - \mathbf{q}_{\text{R},k}\|}$. To quantify the coverage performance, we define the coverage rate as the fraction of spatial locations within the central cell where the received SINR exceeds the target threshold γ_{th}. Specifically, the coverage rate is defined as $R_{\text{cov}} = \frac{1}{N_{\text{grid}}} \sum_{i=1}^{N_{\text{grid}}} \mathbf{1}(\gamma_i > \gamma_{\text{th}})$, where N_{grid} denotes the number of sampled spatial locations in the central cell, and $\mathbf{1}(\cdot)$ denotes the indicator function. The simulation parameters used in this work are summarized in Table I. To compare the coverage performance of different architectures, several simulation cases are considered, including UAV-BS only transmission, AF relay-assisted transmission, passive RIS-assisted transmission, and active RIS-assisted transmission. The detailed parameter values used in each case are summarized in Table II.

Fig. 2. compares the spatial coverage of four architectures. The UAV-BS only and AF relay-assisted schemes provide limited improvement due to the constrained transmit power and dual-hop path loss. Passive RIS expands the coverage through array gain, but the improvement is limited in distant regions because of the cascaded path loss. In contrast, active RIS achieves the widest coverage by combining phase alignment with signal amplification.

Fig. 3. compares the coverage rates of all architectures. The coverage improves with higher relay power in AF relaying and with more reflecting elements in passive RIS. However, active RIS achieves the highest coverage by leveraging both array gain and signal amplification, and with sufficient amplification gain it can fully restore the coverage of the failed base station.

IV. Conclusion

In this paper, we investigated an active RIS-assisted UAV communication system for disaster environments. The coverage probability of four communication architectures—UAV-only, passive RIS-assisted, AF relay-assisted, and active RIS-assisted systems—was evaluated and compared. The results showed that active RIS can mitigate the impact of cascaded path loss in UAV-assisted links through signal amplification, leading to improved coverage performance. These findings demonstrate that active RIS has strong potential for enhancing communication reliability in UAV-assisted disaster recovery networks.

Acknowledgment

This study was carried out with the support of R&D Program for Forest Science Technology '(Project No. RS-2025-25442363)' provided by Korea Forest Service (Korea Forestry Promotion Institute). This work was also supported by the National Research Foundation of Korea (NRF) through the Korean Government (MSIT) under Grant No. RS-2026-25489627.

References

[1] B. Karaman *et al.*, "Solutions for sustainable and resilient communication infrastructure in disaster relief and management scenarios," *IEEE Commun. Surveys Tuts.*, vol. 28, pp. 716–760, Sep. 2026.

[2] M. Matracia, M. A. Kishk, M.-S. Alouini, "UAV-aided post-disaster cellular networks: A novel stochastic geometry approach," *IEEE Trans Veh. Technol.*, vol. 72, no. 7, pp. 9406–9418, Jul. 2023.

[3] S. Barhoumi, M. Erdem, and M. -S. Alouini, "Terahertz band UAV base stations for post-disaster communication," *IEEE Open J. Commun. Soc.*, vol. 6, pp. 4788–4803, May. 2025.

[4] M. Wu, Y. Xiao, Y. Gao, and X. Xiao, "Digital twin for UAV-RIS assisted vehicular communication systems," *IEEE Trans. Wireless Commun.*, vol. 23, no. 7, pp. 7638–7651, Jul. 2025.

[5] Z. Peng, Z. Zhang, C. Pan, M. D. Renzo, O. A. Dobre, and J. Wang, "Beamforming optimization for active RIS-aided multiuser communications with hardware impairments," *IEEE Trans. Wireless Commun.*, vol. 23, no. 8, pp. 9884–9898, Aug. 2025.

[6] Z. Zhang *et al.*, "Active RIS vs. passive RIS: Which will prevail in 6G?," *IEEE Trans. Commun.*, vol. 71, no. 3, pp. 1707–1725, Mar. 2023.

[7] B. Karaman, I. Basturk, E. Zeydan, F. Kara, E. A. Beyazit, S. Taskin, and H. Yanikomeroglu, "HAPS-RIS-assisted IoT networks for disaster recovery and emergency response: Architecture, application scenarios, and open challenges," *arXiv preprint arXiv:2603.17054*, Mar. 2026.